

## RESEARCH ARTICLE

## Coadaptation of the chemosensory system with voluntary exercise behavior in mice

Quynh Anh Thi Nguyen<sup>1</sup>, David Hillis<sup>2</sup>, Sayako Katada<sup>3</sup>, Timothy Harris<sup>2</sup>, Crystal Pontrello<sup>4</sup>, Theodore Garland, Jr.<sup>1,2,5</sup>, Sachiko Haga-Yamanaka<sup>1,2,4\*</sup>

**1** Neuroscience Graduate Program, University of California Riverside, Riverside, California, United States of America, **2** Graduate Program in Genetics, Genomics & Bioinformatics, University of California Riverside, Riverside, California, United States of America, **3** Department of Stem Cell Biology and Medicine, Graduate School of Medical Sciences, Kyushu University, Fukuoka, Japan, **4** Department of Molecular, Cell, and Systems Biology, University of California Riverside, Riverside, California, United States of America, **5** Department of Evolution, Ecology and Organismal Biology, University of California Riverside, Riverside, California, United States of America

\* [sachikoy@ucr.edu](mailto:sachikoy@ucr.edu)



## OPEN ACCESS

**Citation:** Nguyen QAT, Hillis D, Katada S, Harris T, Pontrello C, Garland T, Jr., et al. (2020) Coadaptation of the chemosensory system with voluntary exercise behavior in mice. PLoS ONE 15(11): e0241758. <https://doi.org/10.1371/journal.pone.0241758>

**Editor:** Hiroaki Matsunami, Duke University, UNITED STATES

**Received:** May 20, 2020

**Accepted:** October 20, 2020

**Published:** November 25, 2020

**Copyright:** © 2020 Nguyen et al. This is an open access article distributed under the terms of the [Creative Commons Attribution License](https://creativecommons.org/licenses/by/4.0/), which permits unrestricted use, distribution, and reproduction in any medium, provided the original author and source are credited.

**Data Availability Statement:** The RNA-seq data files are available in the National Center for Biotechnology Information Gene Expression Omnibus (GEO) database (accession identifier GSE146644, (token yrijwgewvhwlluz)).

**Funding:** This work was supported by UCR Initial Complement fund to S.H.Y., and NSF grant DEB-1655362 to T.G. The funders had no role in study design, data collection and analysis, decision to publish, or preparation of the manuscript.

## Abstract

Ethologically relevant chemical senses and behavioral habits are likely to coadapt in response to selection. As olfaction is involved in intrinsically motivated behaviors in mice, we hypothesized that selective breeding for a voluntary behavior would enable us to identify novel roles of the chemosensory system. Voluntary wheel running (VWR) is an intrinsically motivated and naturally rewarding behavior, and even wild mice run on a wheel placed in nature. We have established 4 independent, artificially evolved mouse lines by selectively breeding individuals showing high VWR activity (High Runners; HRs), together with 4 non-selected Control lines, over 88 generations. We found that several sensory receptors in specific receptor clusters were differentially expressed between the vomeronasal organ (VNO) of HRs and Controls. Moreover, one of those clusters contains multiple single-nucleotide polymorphism loci for which the allele frequencies were significantly divergent between the HR and Control lines, i.e., loci that were affected by the selective breeding protocol. These results indicate that the VNO has become genetically differentiated between HR and Control lines during the selective breeding process. Although the role of the vomeronasal chemosensory receptors in VWR activity remains to be determined, the current results suggest that these vomeronasal chemosensory receptors are important quantitative trait loci for voluntary exercise in mice. We propose that olfaction may play an important role in motivation for voluntary exercise in mammals.

## Introduction

Chemical senses are involved in many aspects of behavior. Olfaction is especially important for controlling such intrinsically motivated behaviors as food-seeking, social interactions, and reproductive- and fear-driven behaviors [1]. An ethologically relevant cue is sensed by chemosensory receptors expressed in the sensory organs, which activate a specific neural circuitry for

**Competing interests:** The authors have declared that no competing interests exist.

behavioral motivation and induces an appropriate behavioral output in a specific context [2–5]. Comparative functional studies involving insect model species propose a model wherein molecular evolution of chemosensory receptors is sufficient to induce changes in neural circuit activity and behavioral patterns [6]. Thus, ethologically relevant cues, receptors, neural circuitries, and behavioral habits are likely to evolve together (coadapt) in response to natural and sexual selection.

One olfactory organ, the vomeronasal organ (VNO), occurs in some amphibians, squamates, and some mammals, including rodents. The VNO is known to detect intraspecific signals known as pheromones that trigger behavioral and physiological changes in receivers [2]. Pheromones are non-volatile peptides and small molecular weight compounds that are excreted in such fluids as urine and tears. These molecules are taken up from the environment to the VNO by direct contact and activate the vomeronasal sensory neurons (VSNs) [7, 8]. Generally, each VSN expresses a member of the vomeronasal receptor families: *type 1 vomeronasal receptors (Vmn1rs)*, *type 2 vomeronasal receptors (Vmn2rs)*, and *formyl peptide receptors (Fprs)*, with some exceptions [9–13]. The signals detected by these receptors in the VSNs are axonally sent to glomerular structures and synaptically transmitted to the postsynaptic neurons, also known as mitral-tufted cells, in the accessory olfactory bulb (AOB) [14, 15]. The signals are then processed in the amygdala and hypothalamus, which induce the animal's instinctive behavioral responses and endocrinological changes [2, 16, 17].

Rapid evolution of the receptor genes is a pronounced feature of the vomeronasal system [18–31]. Different species of animals have divergent family members of vomeronasal receptor genes [23, 26–28, 32, 33]. Even within the *Mus musculus* (house mouse) species complex, variation in the coding sequence is frequently observed [18]. Moreover, the abundance of receptor genes expressed in the VNO varies even among different inbred mouse strains [34]. Distributions of single nucleotide polymorphisms (SNPs) observed in lab-derived strains are non-random, and correlated with vomeronasal receptor phylogeny as well as genomic clusters [18]. These observations led us to hypothesize that selective breeding for a behavior that is modulated by chemosensory signals would induce an alteration in genomic clusters of vomeronasal receptors that are potentially involved in the behavior.

Voluntary wheel running (VWR) is an intrinsically motivated behavior, and even wild mice run on a wheel placed in nature [35]. Notably, VWR is one of the most widely studied behaviors in laboratory rodents [36–38]. Individual differences in VWR are highly repeatable on a day-to-day basis, the trait is heritable within outbred populations of rodents, and genes and genomic regions associated with VWR are being identified [39]. Moreover, some of the underlying causes of variation in VWR have been elucidated, in terms of both motivation and ability for voluntary exercise [37, 40, 41]. Importantly, a previous study demonstrated that the presence of conspecific urine increased VWR activity level in adult wild-derived mice [42], suggesting that external chemosensory cues also have a modulatory role in VWR activity.

We have established 4 independent, artificially evolved mouse lines by selectively breeding individuals showing high VWR activity (High Runners; HRs), along with 4 independent, non-selected Control lines over 88 generations [43, 44]. Briefly, all 4 HR lines run ~2.5–3.0-fold more revolutions per day as compared with the 4 Control lines [45, 46]. Studies of mice allowed access to clean wheels or those previously occupied by a different mouse revealed that HRs show higher sensitivity to previously-used wheels and display greater alteration in daily wheel running activities than the Controls [47]. This result suggests that selective breeding for high running activity was accompanied by altered sensitivity to other individuals, suggesting a potential coadaptation of the chemosensory system with voluntary wheel running.

In this study, we examined whether selective breeding for VWR has differentiated the vomeronasal receptor genes between HR and Control lines. We found that a repertoire of receptor

genes was differentially expressed between the VNO of HR and Control lines, which resulted from reduction or increase of specific vomeronasal receptor-expressing cells in the VNO of HR lines. We also found that this gene expression change was partially due to the genetic alteration upon selective breeding for VWR, suggesting a relationship between high running activity and the function of the VNO in HR lines. Taken together, our results indicate vomeronasal receptors as quantitative trait loci (QTL) for voluntary exercise behavior in mice.

## Results

### Differential expression of vomeronasal receptors in the VNO of HR and Control lines

To examine the impact of selective breeding for VWR activity on receptor gene expression in the VNO, we conducted transcriptome analysis of the VNO from both males and females of HR and Control lines. For each sex and replicate line of the 4 HR and 4 Control lines, total RNA samples were prepared, each consisting of the combined VNOs from 3 individual mice. After RNA sequencing, we identified 132 differentially expressed (DE) genes in the HR line group compared to the Control line group (Fig 1). We identified 19 vomeronasal receptor genes in the DE gene set, which belong to either the *Fpr*, *Vmn1r* or *Vmn2r* family (Fig 1, shown in red). Of the 19 DE receptor genes, the Reads Per Kilobase Million (RPKM) of *Fpr3*, *Fpr-rs4*, *Vmn2r8*, *Vmn2r9*, *Vmn2r11*, *Vmn2r96*, *Vmn2r98*, *Vmn2r102*, *Vmn2r107*, *Vmn2r110*, and *Vmn2r114* were significantly up-regulated, while *Vmn1r188*, *Vmn1r236*, *Vmn2r13*, *Vmn2r15*, *Vmn2r16*, *Vmn2r23*, *Vmn2r45*, and *Vmn2r99* were significantly down-regulated in the VSNs of HR lines compared to Control lines (Fig 2A). The RPKM of *olfactory marker protein (OMP)*, which is abundantly and exclusively expressed in all mature VSNs in the VNO [48], was not different between HR and Control lines (data not shown), indicating that receptor gene expression changes were not due to variation in VSN number. The  $\log_2$  fold change of normalized expression of the DE genes varied from -3.3 to 2.1 (Fig 2B). *Fpr-rs4* and *Vmn2r16* showed the largest upregulation and downregulation, respectively. To examine sexually-biased expressions, we separated RPKMs of each DE receptor gene into sex and linetype groups (S1 Fig) and performed a two-way ANOVA test to examine sex and linetype differences. As shown in S2 Fig, *p* values for sexually-biased expression and interaction were above 0.05 in all DE receptor genes, demonstrating that there are no sex-dimorphic expression changes between HR and Control lines. These results suggest that expression of the chemosensory receptor genes is differentially regulated in the VSNs between HR and Control lines without a sex difference.

Interestingly, 15 out of 19 DE receptor genes are co-localized in specific vomeronasal receptor clusters. *Vmn2r8*, *Vmn2r9*, *Vmn2r11*, *Vmn2r13*, *Vmn2r15*, and *Vmn2r16* are localized in a ~1 Mb vomeronasal receptor cluster on chromosome 5, and *Fpr3*, *Fpr-rs4*, *Vmn2r96*, *Vmn2r98*, *Vmn2r99*, *Vmn2r102*, *Vmn2r107*, *Vmn2r110*, and *Vmn1r236* are localized in a ~3 Mb vomeronasal receptor cluster on chromosome 17 (Fig 3). *Vmn2r23*, *Vmn2r45*, *Vmn1r188*, and *Vmn2r114* exist on chromosome 6, 7, 10, and 17, respectively (Fig 3), and they are surrounded by vomeronasal receptors which are not differentially expressed between HR and Control lines. These results suggest the correlation of differential expression of vomeronasal receptors and genomic chromosomal locations, as well as other unknown causes.

### Accumulation of all-or-none SNPs in a vomeronasal receptor cluster

We then hypothesized that differences between HR and Control lines in vomeronasal receptor gene expression may be associated with differences in genomic sequences, especially allele

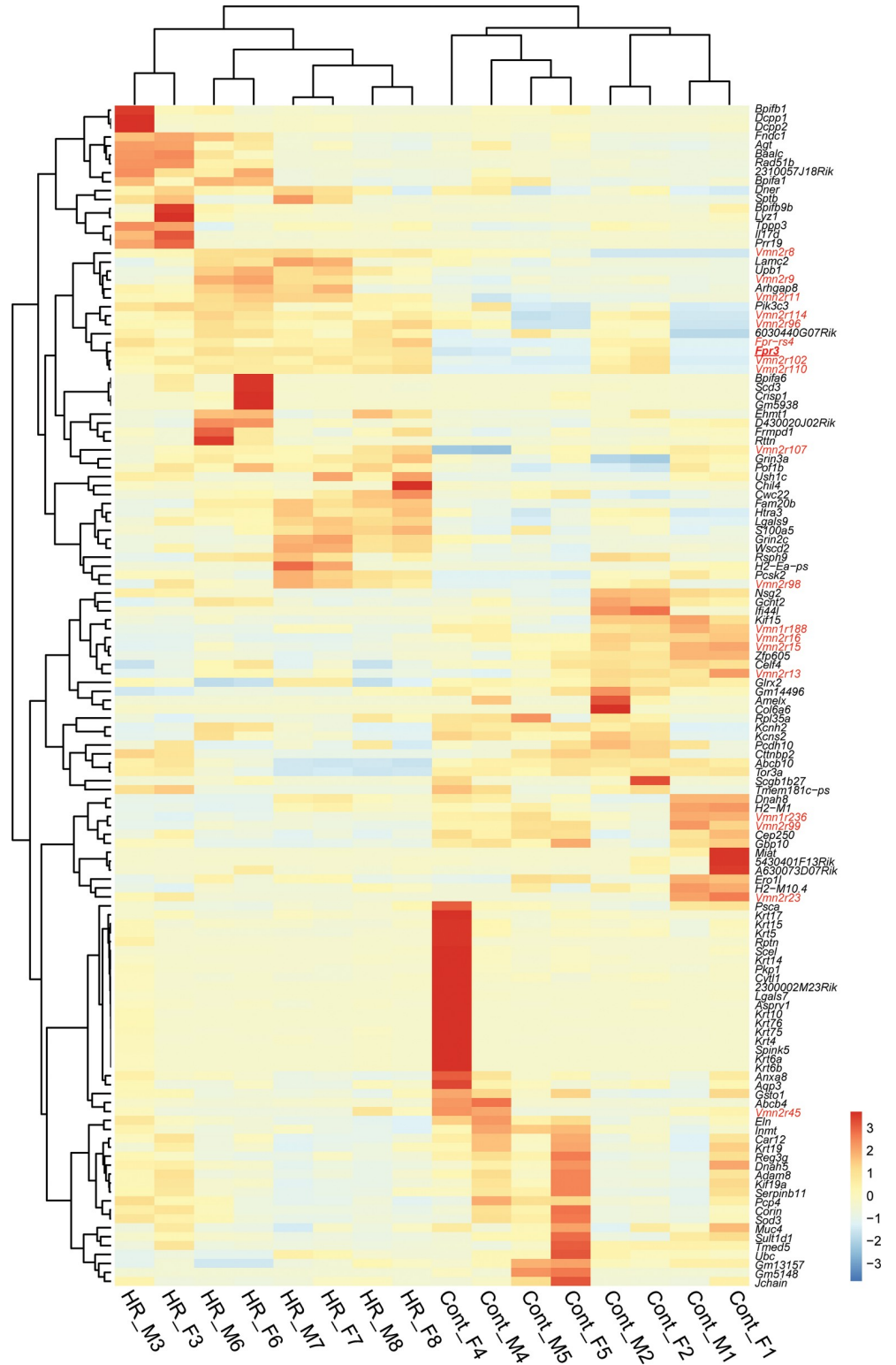


**Fig 1. RNAseq analysis of the vomeronasal organs of High Runner and Control mice.** Heatmap of differentially expressed (DE) genes between HR and Control lines. DE vomeronasal receptors are shown in red. *Fpr3* (analyzed in Fig 5) is highlighted with a red underline.

<https://doi.org/10.1371/journal.pone.0241758.g001>

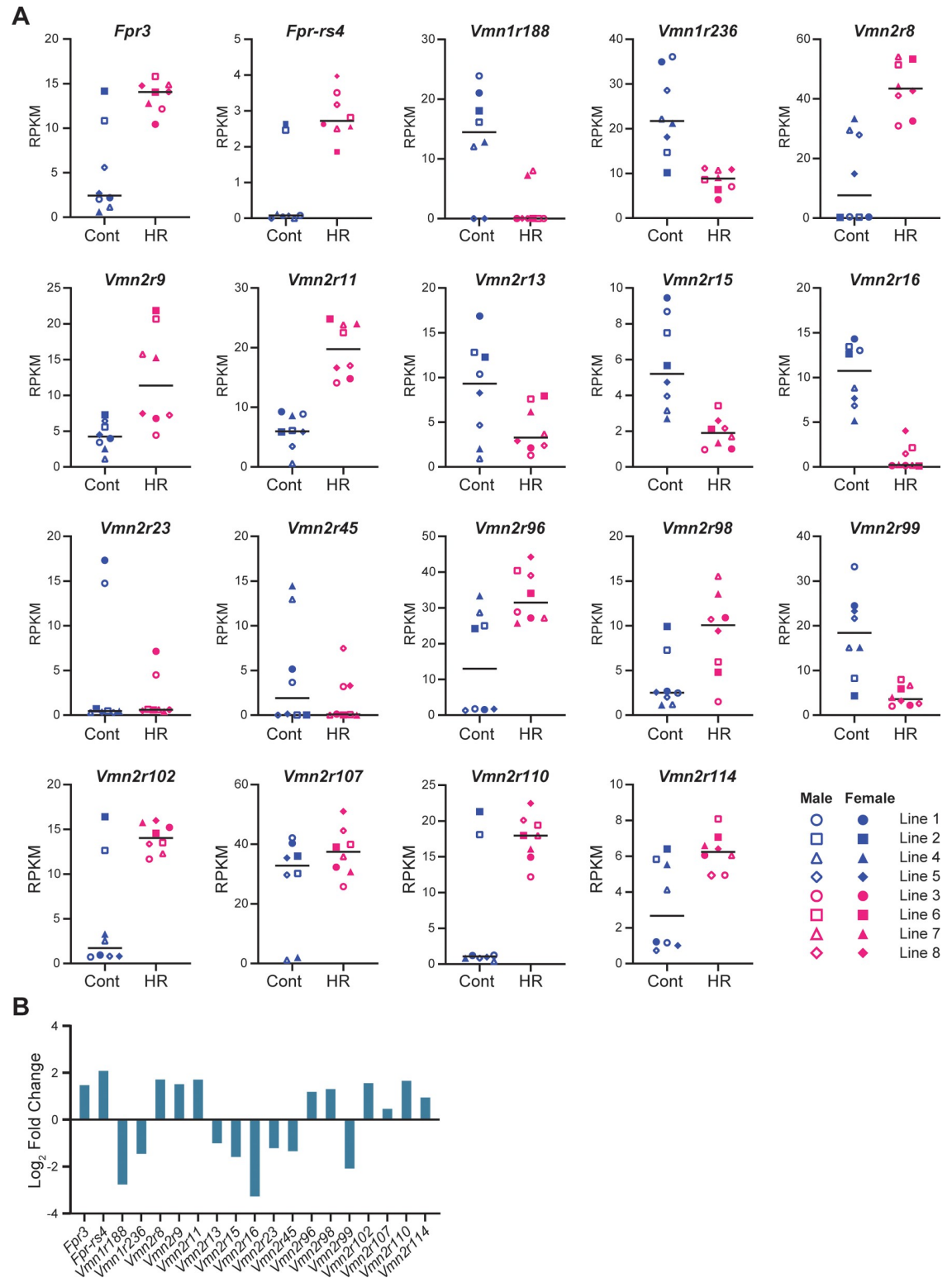


**Fig 2. RPKM comparison of DE vomeronasal receptors between High Runner and Control mice.** (A) Scatter plots showing the RPKM of DE vomeronasal receptor genes in each line of HR or C mice. Black bars represent medians. (B) Bar graph denoting  $\log_2$  fold change of the relative expression of DE vomeronasal receptor genes between the HR and Control lines.

<https://doi.org/10.1371/journal.pone.0241758.g002>

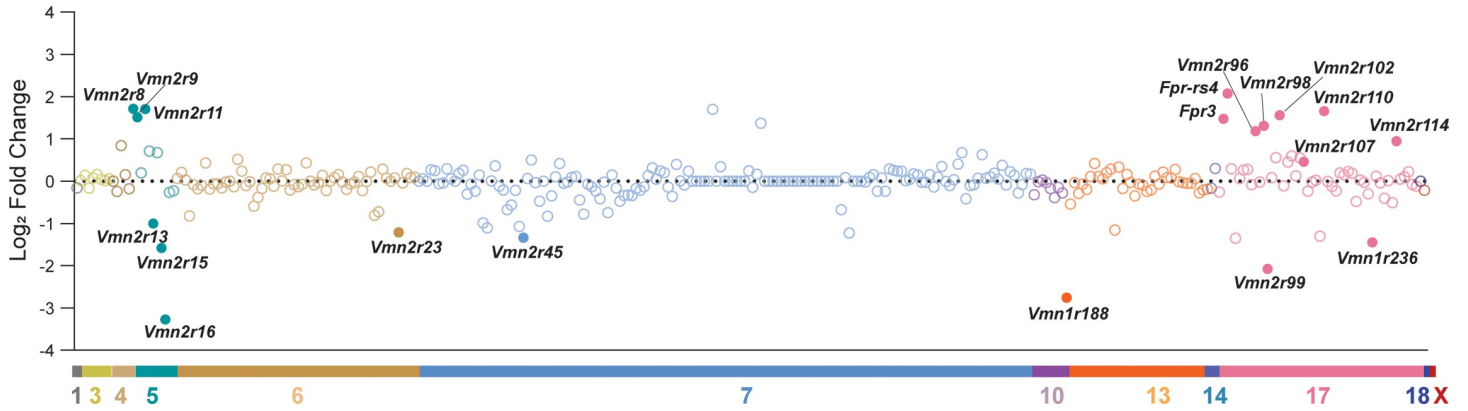


**Fig 3. Chromosomal locations of DE vomeronasal receptors.** A plot showing the log<sub>2</sub> fold change of 336 vomeronasal receptor genes in their relative positions along the chromosomes. Each circle represents a member of *Vmn1r*, *Vmn2r*, or *Fpr* family genes. DE vomeronasal receptors are shown in filled circles.

<https://doi.org/10.1371/journal.pone.0241758.g003>

frequencies between HR and Control lines caused by the selective breeding. Previous genome-wide SNP analysis detected 152 out of 25,318 variable SNP loci for which allele frequencies are significantly different between HR and Control lines after correction for multiple comparisons [49]. As explained in the previous paper, the differentiation in allele frequencies for these 152 loci cannot be attributed to random genetic drift. Of the 152 SNP loci, we particularly focused on 61 loci that are fixed for the same allele in all 4 replicate HR lines but not fixed in any of the 4 replicate Control lines, or vice versa (which we term “all-or-none SNPs”, S1 Table). The 61 SNP loci are not randomly distributed throughout the genome (S3A Fig). The majority of them (59 of 61) exist as a member of groups of 3 or more which are located in close proximity on the genomic chromosomes (S3B Fig). As a result, only 11 all-or-none SNP clusters are observed in the genome (S3A Fig)

Interestingly, 8 of the 61 all-or-none SNP loci are located in a ~3 Mb interval on chromosome 17 that contains clusters of *Vmn1rs* (14), *Vmn2rs* (21), and *Fprs* (7) (Fig 4). Strikingly, 9 out of the 19 DE vomeronasal receptors are located in this all-or-none SNP cluster. Five of the all-or none SNPs are localized near the differentially expressed vomeronasal receptors (Table 1): SNP ID rs29503987 at 30 kb downstream and 20 kb upstream of *Fpr3* and *Fpr-rs4*, respectively, rs33447983 at 8.4 kb downstream of *Vmn2r99*, rs6224641 at 30 kb downstream of *Vmn2r99*, rs33649277 at 44 kb upstream of *Vmn2r102*, rs29522462 at 524 bp downstream of *Vmn2r110*, and rs33120398 at the intron 1 of *Vmn2r110*. Other SNPs, such as rs33463529, are

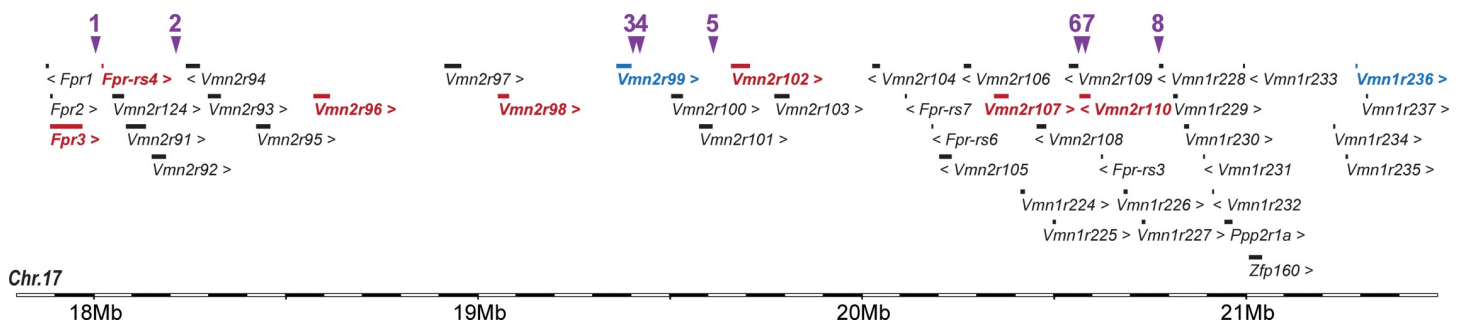


**Fig 4. A genomic cluster containing both SNPs and DE vomeronasal receptors.** A genomic cluster containing DE vomeronasal receptor genes in the mouse chromosomes 17. Vomeronasal receptors in red and blue indicate up- and down-regulations, respectively. Non-DE genes are shown in black. Purple arrowheads indicate locations of SNPs that are significantly differentiated between HR and Control groups [49], as shown in Table 1.

<https://doi.org/10.1371/journal.pone.0241758.g004>

**Table 1. Locations of SNPs on the chromosome 17 that are significantly differentiated between HR and Control groups.**

	SNP ID	SNP location (mm10)	HR / Cont	Gene (within 50kb)	strand	up/dw	Distance (bp)
1	rs29503987	18001459	C / A	<i>Fpr-3</i>	+	dw	29935
				<i>Fpr-rs4</i>	+	up	20274
				<i>Vmn2r124</i>	+	up	48025
2	rs33375308	18210739	T / C	<i>Vmn2r92</i>	+	dw	25561
3	rs33447983	19403011	G / T	<i>Vmn2r99</i>	+	dw	8421
4	rs6224641	19424358	A / G	<i>Vmn2r99</i>	+	dw	29768
5	rs33649277	19616228	G / A	<i>Vmn2r101</i>	+	dw	3911
				<i>Vmn2r102</i>	+	up	44171
6	rs29522462	20573305	A / C	<i>Vmn2r109</i>	-	up	8549
				<i>Vmn2r110</i>	-	dw	524
7	rs33120398	20587484	C / T	<i>Vmn2r109</i>	-	up	22728
				<i>Vmn2r110</i>	-	intron 1	
				<i>Fpr-rs3</i>	-	dw	36362
8	rs33463529	20779567	G / A	<i>Vmn1r227</i>	+	dw	43441
				<i>Vmn1r228</i>	-	up	2066
				<i>Vmn1r229</i>	+	up	34928

<https://doi.org/10.1371/journal.pone.0241758.t001>

also closely located near vomeronasal receptors, though changes in expression of the nearby receptors were not observed. These results strongly suggest that changes in vomeronasal receptor gene expression between HR and Control lines are at least partially caused by changes in allele frequencies at multiple loci in response to selective breeding for VWR activity.

The rest of the DE vomeronasal receptors, which are located in another vomeronasal receptor cluster on chromosome 5, as well as other solitary ones, are not surrounded by SNP loci that are significantly differentiated between HR and Control lines [49]. Therefore, expression changes of the receptor genes may be mediated by SNPs that remain polymorphic in both lines, or by different mechanisms.

### Differential number of *Fpr3*-expressing VSNs in the VNO of HR and Control lines

To determine the significance at the cellular level in the VNO of the DE chemosensory receptor genes, we chose one representative gene to determine whether there are differences in the number of receptor-expressing VSNs, or alternatively, differences in transcript abundance in each receptor-expressing VSN. We performed *in situ* hybridization to detect *Fpr3* in the VNO of 2–3 individual mice from each of the 4 HR and 4 Control lines, together with a probe for the *Gao* (*Gnao1*). Expression of *Fpr3* is ~3 times higher in HR lines compared to Control lines in RNAseq analysis (Fig 2B). Although *Fpr3*-expressing VSNs were observed in the VNO of both HR and Control lines, the number of *Fpr3*-expressing VSNs in each VNO slice varied among lines (Fig 5A and 5B). In 3 Control lines (line 1, 4, and 5), *Fpr3* signal was barely observed in each VNO tissue slice, while Control line 2 had a significantly higher number of *Fpr3*-expressing VSNs (Fig 5B). This result was consistent with the RNAseq data, in which the amount of *Fpr3* transcripts in line 2 was higher than other Control lines (Fig 2A). We consistently observed multiple *Fpr3*-expressing VSNs in most of the VNO tissue slices from the 4 HR lines and Control line #2 (Fig 5B and 5C). Generally, there were significantly more *Fpr3*-expressing VSNs in the HR versus the Control lines (Fig 5C, Mann-Whitney test ( $p < 0.05$ )). The fluorescent intensity derived from *Fpr3* gene transcripts in each VSN was not distinguishable between the VNO tissues from HR and Control lines (Fig 5D and 5E). Taken together,

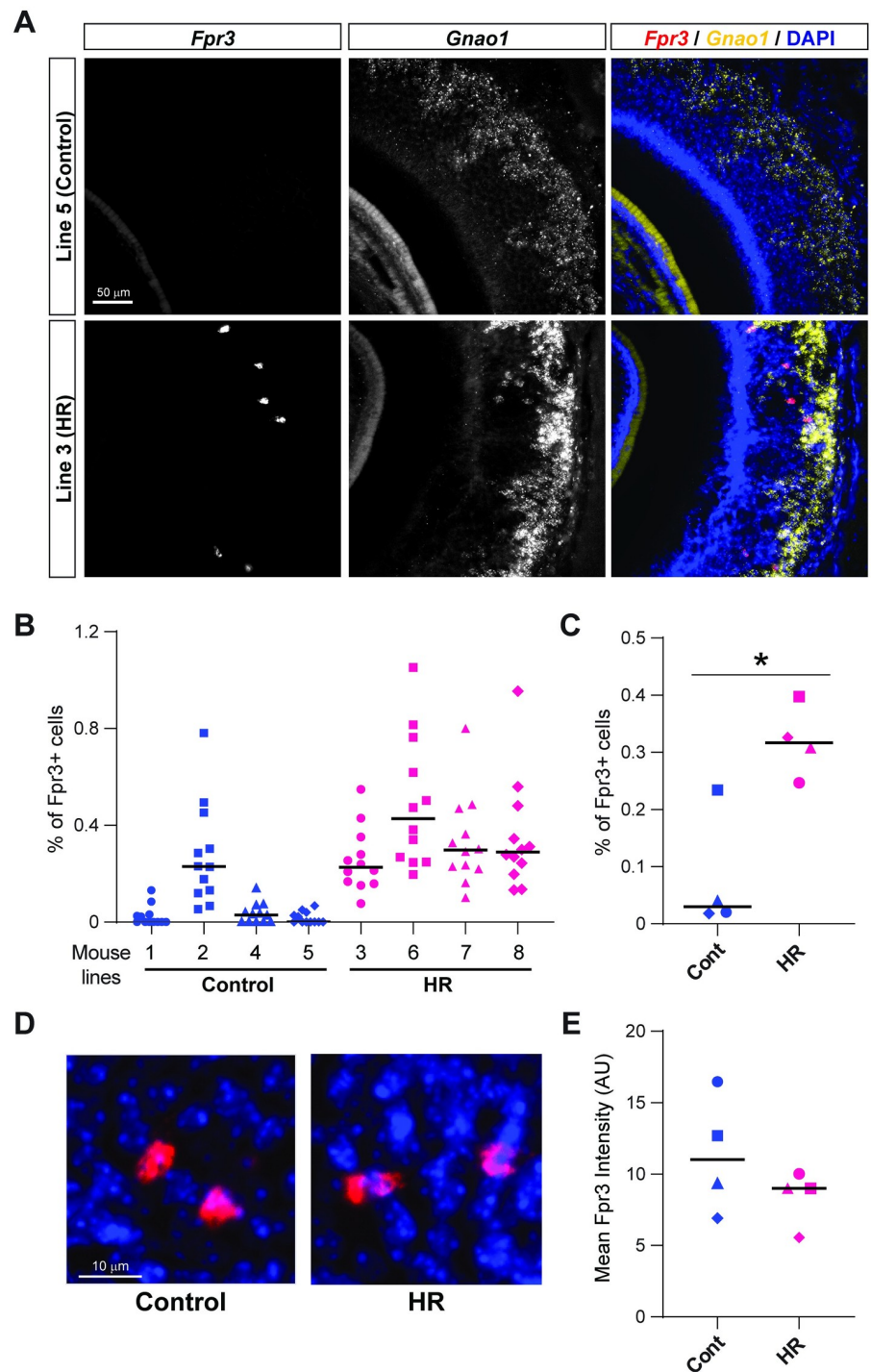


**Fig 5. RNA scope *in situ* hybridization analysis of a DE vomeronasal receptor gene in the VNO.** (A) Images showing RNAscope-derived fluorescent signals for *Fpr3* (left) and *Gnao1* (middle) transcripts. In merged images (right), *Fpr3* and *Gnao1* are shown in red and yellow, respectively, together with DAPI staining (blue). Upper and lower panels show representative images from the VNO of a Control (line 5) line and a HR (line 3) line, respectively. (B) A scatter plot showing the percentage of *Fpr3* signals in vomeronasal sensory neurons (VSNs) per VNO slice for each line of mice.  $n = 12$  slices in 2–3 mice per line. Black bars represent medians. (C) The mean percentage of *Fpr3* signals in VSNs in Control and HR lines. Each dot indicates the mean of one line. Black bars represent medians. \* indicates  $p < 0.05$  in Mann-Whitney test. (D) Representative images showing *Fpr3* signals (red) observed in the VNO of Control and HR lines of mice. DAPI signals are shown in blue. (E) The mean of *Fpr3* signal intensity (arbitrary unit, AU) per VSN in the Control and HR lines. Each dot indicates the mean of one line. Black bars represent medians.

<https://doi.org/10.1371/journal.pone.0241758.g005>



these results demonstrate that the different expression levels of the chemosensory receptors result from changes in the number of the receptor-expressing VSNs. The results observed here are consistent with a previous finding in the main olfactory system, which has a similar mono-allelic pattern of receptor gene expression in each sensory neuron [50]: a positive correlation between tissue RNA levels of olfactory receptor genes and numbers of OSNs expressing the receptors. Thus, the number of VSNs expressing specific sets of chemosensory receptors are differentially regulated after selective breeding for VWR.

## Discussion

In this study, we utilized a unique animal model: 4 replicate mouse lines that have been experimentally evolved by selectively breeding individuals showing high VWR activity (HR lines), along with their 4 independent, non-selected Control lines maintained over 88 generations [43]. The HR and Control lines provide a strong model for determining the contribution of genetics to voluntary-exercise related traits [44, 51]. In addition to the exercise ability-related genetic adaptations found after selective breeding [37, 44], several changes at the level of the central nervous system have also been identified, which contribute to elevation of VWR for HR mice [37, 40, 52]. Through SNP mapping analysis (S1 Fig), we found that 3 of the 61 all-or-none SNP loci that were fixed in all 4 replicate HR lines (but none of the 4 replicate Control lines) were located in a genomic cluster exclusively containing T-box genes on Chromosome 5. These genes are associated with GO terms of “bundle of His development,” “embryonic forelimb morphogenesis,” “cardiac septum morphogenesis,” “ventricular septum development,” and “cardiac muscle cell differentiation”. Indeed, compared with their 4 non-selected Control line counterparts, mice from the 4 replicate HR lines have been shown to have increased ventricular mass [45, 53–55], as well as altered cardiac functions [55–57]. Thus, the genome-wide SNP analysis of HR and Control lines of mice [49] could robustly identify QTL associated with voluntary exercise behavior.

Vomeroneasal receptors are among the most rapidly evolving genes in vertebrates [18–31]. Different taxonomic groups have divergent family members of vomeronasal receptor genes [21, 23, 26–28, 32, 33], and the abundance of receptor genes expressed in the VNO is different even among inbred mouse strains [34]. Moreover, many of the mouse pheromones identified as ligands for vomeronasal receptors show strain specificity. For example, expression of the male pheromone ESP1 is only observed in a few inbred strains, although males of wild-derived strains all secrete abundant ESP1 peptide into their tears [58]. Likewise, expression of juvenile pheromone ESP22 is missing in some inbred strains [59]. Major urinary proteins (MUPs) are potential ligands for vomeronasal receptors, and all male mice of a given inbred strain secrete identical MUP members, whereas wild-derived mice each exhibit a unique profile of emitted MUPs [60]. Thus, pheromones and receptors in the vomeronasal system may have evolved in response to various environmental changes, including domestication, which resulted in alteration of coding sequences and expression patterns.

Considering the extensive evolution of receptor genes, selective breeding for a chemosensory-mediated behavior is an attractive alternative approach to reveal the functions of vomeronasal receptors. VWR activity of a mouse strain that recently derived from the wild has been shown to be increased by urinary chemosignals from other individuals [42]. Therefore, if the function of the VNO is involved in the modulation of VWR activity, then we would expect that selective breeding for high VWR activity should impact vomeronasal receptors. Indeed, we found that expression levels of several vomeronasal receptor genes as well as a few SNPs near the DE receptor genes were different between HR and Control lines. Although the role of each DE receptor in VWR activity needs to be determined in future studies, the current results

suggest that vomeronasal chemosensory receptors could be important QTLs for voluntary exercise in mice.

One of the important remaining questions is how the vomeronasal system modulates VWR behavior in HR lines. One study measuring patterns of brain activity using *c-Fos* immunoreactivity revealed multiple areas in the brain that appear to be associated with motivation for VWR in HR lines [61]. These areas include brain nuclei known to be motivation-related, such as the prefrontal cortex, medial frontal cortex, and nucleus accumbens (NAc) [61]. In addition, it was recently shown in mice that VNO-mediated signals regulate the mesolimbic dopaminergic system, especially by upregulating the ventral tegmental area (VTA)-NAc circuit, and that they enhance reproductive motivation in mice [15]. Thus, it is possible that the VNO-mediated chemosensory signals also upregulate VWR activity by stimulating the VTA-NAc circuit. Moreover, one of the hypothalamic targets of the vomeronasal system, the medial preoptic area (MPOA), has been shown to regulate wheel-running activity in a hormone-dependent manner [62–65]. It is therefore also conceivable that the VNO-mediated chemosensory signals upregulate VWR by directly activating MPOA neurons. Combined with these previous observations, we propose that chemosensory signals detected by the VNO activate specific areas of the central nervous system that contribute to VWR activity. Future studies are expected to reveal the role of the VNO in modulating physical exercise and other voluntary behaviors in rodents.

## Materials and methods

### Animals

The experimental procedures were approved by the UCR Institutional Animal Care and Use Committee and were in accordance with the National Institutes of Health Guide for the Care and Use of Laboratory Animals. The VNOs studied were from 12-week old male and female mice of 4 lines selected for high voluntary wheel running and 4 Control lines. The studied mice were derived from generation 88 of a replicated selective breeding experiment for increased voluntary wheel running behavior that began with a base population of the outbred Hsd:ICR strain [43]. Wheel revolutions were recorded in 1-minute intervals continuously for 6 days, and mice were selected within-family for the number of revolutions run on days 5 and 6. In each selected HR line, the highest-running male and female within 10 individual families were selected per generation and each mouse was mated to a mouse from another family, within its line. This within-family selection regimen minimized inbreeding such that the effective population size was approximately 35 in each line [43]. In the Control lines, one female and one male within each family were chosen at random, though full sibling mating was again prevented. The mice in the present study were neither full nor half-siblings.

### RNA sequencing

The VNO tissues were harvested from 3 male and 3 female mice from each of the 4 HR and 4 Control lines, immediately transferred to RNA later (Sigma-Aldrich), then stored at  $-80^{\circ}\text{C}$  until use for RNA-seq. VNO tissues from the same sex and line of mice were pooled and homogenized in Trizol Reagent (Life Technologies, Carlsbad, CA) and processed according to the manufacturer's protocol. Trizol-purified RNA samples were quantified using Qubit1 2.0 (Life Technologies). The integrity of isolated RNA was measured by the 28S/18S rRNA analysis using the Agilent 2100 Bioanalyzer (Agilent Technologies, Santa Clara CA) with RNA Nano chip (Agilent Technologies, Palo Alto, CA). Samples had RNA integrity number values of at least 8.30. Using the Ultra II Directional RNA Library Prep kit (NEB), each RNA sample was depleted of ribosomal RNA and used to prepare an RNA-seq library tagged with a unique

barcode at the UCR IIGB Genomics Core. Libraries were evaluated and quantified using Agilent 2100 Bioanalyzer with High Sensitivity DNA chip, then sequenced with the Illumina Next-Seq 500 system (Illumina, San Diego, CA, USA) and 75nt-long single-end reads were generated at the UCR IIGB Genomics Core. A total of 8 libraries (4 HR lines and 4 Control lines) were multiplexed and sequenced in a single lane which yielded ~11,000 M reads, averaging ~1,400 M reads per sample.

The RNA-seq data files are available in the National Center for Biotechnology Information Gene Expression Omnibus (GEO) database (accession identifier GSE146644).

### Differential gene expression analysis

The analysis compared the transcriptome profiles from both males and females of the HR and Control lines of mice. Quality control of the sequence reads included a minimum average Phred score of 30 across all positions using FastQC. Sequencing reads were aligned to the mouse reference genome (GRCm38/mm10), using STAR aligner ver. 2.6.1d [66] with an increased stringency unforbearing any of mismatches per each read ('-outFilterMismatchNmax 0'). Any reads that map to multiple locations in the genome are not counted ('-outFilterMulti-mapNmax 1') since they cannot be assigned to any gene unambiguously. In order to determine the differentially expressed (DE) genes, generated BAM files were accessed with Cuffdiff [67], a program included in Cufflinks. Cuffdiff reports reads per kp per million mapped reads (RPKM),  $\log_2$  fold change, together with  $p$ -value, and adjusted  $p$ -values ( $q$ -values). After Benjamini-Hochberg false discovery correction, genes with  $q$ -values less than 0.05 were considered as DE genes. To examine sexual differences, RPKM of DE vomeronasal receptor genes in male and female HR and Control mice were subjected to two-way ANOVA tests using Prism (GraphPad). Notably,  $p$ -values for linetype-biased expression of 4 DE receptor genes (Vmn2r13, Vmn2r23, Vmn2r45, and Vmn2r107) were  $> 0.05$  due to differences of statistical tests: the negative binomial regression in DE gene detection and the general linear model in two-way ANOVA.

### Analysis of all-or-none SNPs

SNP data in supplemental table 7 (Data\_S7) in Xu and Garland (2017) [49] were used for this analysis. SNPs that separate all 4 HR and 4 Control lines (which we term all-or-none SNPs) were selected (S1 Table) and mapped onto mouse genome (NCBI37/mm9) using UCSC Genome Browser (<https://genome.ucsc.edu>). We noticed that most of the all-or-none SNPs occurred in groups. Thus, we mapped those SNP clusters onto genomes (S3A Fig). Each cluster was defined—and + 0.1 Mb from the first and last SNP, respectively, observed in a specific location of the genome. Information of coding genes in each SNP cluster were extracted (S3B Fig). For some clusters, Gene-to-GO mappings was performed with PANTHER (<http://pantherdb.org>).

### RNAscope *in situ* hybridization

Female mice (11 Controls and 10 HRs) were utilized for this analysis. The animals were intracardially perfused with 4% Paraformaldehyde in Phosphate Buffered Saline (PBS). VNOs were dissected from perfused animals and fixed overnight. The VNO samples were decalcified in EDTA pH 8.0 for 48 hours, then cryoprotected in 15% sucrose in PBS followed by 30% sucrose in PBS. All samples were ultimately embedded in optimal cutting temperature (OCT) medium (Electron Microscopy Sciences) above liquid nitrogen and sectioned at 20  $\mu\text{m}$  using Leica CM3050S Cryostat. The cross sections analyzed were from the VNO regions with clearly discernible two crescent shapes. They were collected approximately 120  $\mu\text{m}$  apart from each

other spanning approximately 360  $\mu\text{m}$  of the VNO containing regions from each mouse. Slides were stored at  $-80^{\circ}\text{C}$  until use for *in situ* hybridization staining.

RNA detection in VNOs were performed with ACD RNAscope<sup>®</sup> control and target GNAO1 (ACD # and FPR3 (ACD #503451) using RNAscope<sup>®</sup> Multiplex Fluorescent Reagent Kit v2 (ACD# 323100) Assay. Probe binding was detected with Akoya Biosciences' Opal 690 (FP1497001KT) and 570 (FP1488001KT) Dyes at 1:750 dilution in RNAscope TSA Buffer. Nuclear staining was visualized with DAPI (EMS #17989–20). Images were acquired at 20X or 40X magnification on Zeiss Axio Imager.M2, and FPR3-positivity was quantified with a proprietary script using QuPath software [68]. Fluorescent intensity was measured by Fiji software. 4–8 slices in each animal were examined. Mann-Whitney test was used to examine statistical significance in Fig 5C and 5E.

## Supporting information

**S1 Fig. RPKM comparison of DE vomeronasal receptors between males and females in High Runner and Control mice.** Scatter plots showing the RPKM of DE vomeronasal receptor genes in males and females from each line of HR or Control mice. Black bars represent medians.

(TIF)

**S2 Fig. Two-way ANOVA tests of DE vomeronasal receptors.** A table showing *p*-values for interactions, sex differences, and linetype differences in the RPKM of DE vomeronasal receptor genes in two-way ANOVA analyses. n.s., \*, \*\*, \*\*\*, and \*\*\*\* represent not significant,  $p < 0.05$ ,  $p < 0.01$ ,  $p < 0.001$ , and  $p < 0.0001$ , respectively.

(TIF)

**S3 Fig. Analysis of all-or-none SNP loci in HR and Control lines of mice.** (A) A schematic diagram showing the relative positions of loci containing 1 or more all-or-none SNPs. Blue triangles indicate non-chemosensory clusters, and a red triangle indicates clusters containing only chemosensory (vomeronasal) receptors. (B) A table showing chromosomal location and length of each all-or-non SNP cluster, and the number of SNPs and genes within the clusters. The row highlighted in red is the cluster containing only the vomeronasal receptor genes.

(TIF)

**S1 Table. Genomic locations, *p*-value by the mixed model approach [49], and allele frequencies of the 61 all-or-on SNP loci.**

(XLSX)

## Acknowledgments

We thank Drs C. R. Yu, H. Matsunami, T. Girke, P. Campbell, C. A. Scott and N. Yamanaka for helpful discussions and comments on the manuscript. We are grateful for technical assistance from Office of Campus Veterinarian, and Genomics Core Facility at University of California, Riverside (UCR).

## Author Contributions

**Conceptualization:** Theodore Garland, Jr., Sachiko Haga-Yamanaka.

**Data curation:** Sachiko Haga-Yamanaka.

**Formal analysis:** Quynh Anh Thi Nguyen, Sayako Katada.

**Funding acquisition:** Theodore Garland, Jr., Sachiko Haga-Yamanaka.

**Investigation:** Quynh Anh Thi Nguyen, Sayako Katada.

**Methodology:** Quynh Anh Thi Nguyen, David Hillis, Timothy Harris, Crystal Pontrello.

**Resources:** Theodore Garland, Jr.

**Supervision:** Theodore Garland, Jr., Sachiko Haga-Yamanaka.

**Validation:** Theodore Garland, Jr., Sachiko Haga-Yamanaka.

**Visualization:** Sachiko Haga-Yamanaka.

**Writing – original draft:** Sachiko Haga-Yamanaka.

**Writing – review & editing:** Sayako Katada, Crystal Pontrello, Theodore Garland, Jr., Sachiko Haga-Yamanaka.

## References

1. Nielsen BL. Olfaction in animal behaviour and welfare: CABI; 2017 2017/6/29. 233 p.
2. Liberles SD. Mammalian pheromones. *Annu Rev Physiol.* 2014; 76(1):151–75. <https://doi.org/10.1146/annurev-physiol-021113-170334> PMID: 23988175
3. Mohrhardt J, Nagel M, Fleck D, Ben-Shaul Y, Spehr M. Signal Detection and Coding in the Accessory Olfactory System. *Chem Senses.* 2018; 43(9):667–95. <https://doi.org/10.1093/chemse/bjy061> PMID: 30256909
4. Ishii KK, Touhara K. Neural circuits regulating sexual behaviors via the olfactory system in mice. *Neurosci Res.* 2019; 140:59–76. <https://doi.org/10.1016/j.neures.2018.10.009> PMID: 30389572
5. Fleischer J, Krieger J. Insect Pheromone Receptors—Key Elements in Sensing Intraspecific Chemical Signals. *Front Cell Neurosci.* 2018; 12:425. <https://doi.org/10.3389/fncel.2018.00425> PMID: 30515079
6. Cande J, Prud'Homme B, Gompel N. Smells like evolution: the role of chemoreceptor evolution in behavioral change. *Curr Opin Neurobiol.* 2013; 23(1):152–8. <https://doi.org/10.1016/j.conb.2012.07.008> PMID: 22884223
7. Halpern M. The organization and function of the vomeronasal system. *Annu Rev Neurosci* 1987; 10(1):325–62. <https://doi.org/10.1146/annurev.ne.10.030187.001545> PMID: 3032065
8. Halpern M. Structure and function of the vomeronasal system: an update. *Prog Neurobiol.* 2003; 70(3):245–318. [https://doi.org/10.1016/s0301-0082\(03\)00103-5](https://doi.org/10.1016/s0301-0082(03)00103-5) PMID: 12951145
9. Dulac C, Axel R. A novel family of genes encoding putative pheromone receptors in mammals. *Cell.* 1995; 83(2):195–206. [https://doi.org/10.1016/0092-8674\(95\)90161-2](https://doi.org/10.1016/0092-8674(95)90161-2) PMID: 7585937
10. Herrada G, Dulac C. A novel family of putative pheromone receptors in mammals with a topographically organized and sexually dimorphic distribution. *Cell.* 1997; 90(4):763–73. [https://doi.org/10.1016/s0092-8674\(00\)80536-x](https://doi.org/10.1016/s0092-8674(00)80536-x) PMID: 9288755
11. Matsunami H, Buck LB. A multigene family encoding a diverse array of putative pheromone receptors in mammals. *Cell.* 1997; 90(4):775–84. [https://doi.org/10.1016/s0092-8674\(00\)80537-1](https://doi.org/10.1016/s0092-8674(00)80537-1) PMID: 9288756
12. Rivière S, Challet L, Fluegge D, Spehr M, Rodriguez I. Formyl peptide receptor-like proteins are a novel family of vomeronasal chemosensors. *Nature.* 2009; 459(7246):574–7. <https://doi.org/10.1038/nature08029> PMID: 19387439
13. Liberles SD, Horowitz LF, Kuang D, Contos JJ, Wilson KL, Siltberg-Liberles J, et al. Formyl peptide receptors are candidate chemosensory receptors in the vomeronasal organ. *Proc Natl Acad Sci U S A.* 2009; 106(24):9842–7. <https://doi.org/10.1073/pnas.0904464106> PMID: 19497865
14. Wagner S, Gresser AL, Torello AT, Dulac C. A multireceptor genetic approach uncovers an ordered integration of VNO sensory inputs in the accessory olfactory bulb. *Neuron.* 2006; 50(5):697–709. <https://doi.org/10.1016/j.neuron.2006.04.033> PMID: 16731509
15. Ben-Shaul Y, Katz LC, Mooney R, Dulac C. In vivo vomeronasal stimulation reveals sensory encoding of conspecific and allospecific cues by the mouse accessory olfactory bulb. *Proc Natl Acad Sci U S A.* 2010; 107(11):5172–7. <https://doi.org/10.1073/pnas.0915147107> PMID: 20194746
16. Meredith M. Vomeronasal, Olfactory, Hormonal Convergence in the Brain: Cooperation or Coincidence? *Ann N Y Acad Sci.* 1998; 855(1 OLFACTION AND):349–61. <https://doi.org/10.1111/j.1749-6632.1998.tb10593.x> PMID: 9929627

17. Tirindelli R, Dibattista M, Pifferi S, Menini A. From pheromones to behavior. *Physiol Rev*. 2009; 89(3):921–56. <https://doi.org/10.1152/physrev.00037.2008> PMID: 19584317
18. Wynn EH, Sánchez-Andrade G, Carss KJ, Logan DW. Genomic variation in the vomeronasal receptor gene repertoires of inbred mice. *BMC Genomics*. 2012; 13:415. <https://doi.org/10.1186/1471-2164-13-415> PMID: 22908939
19. Zhang J, Webb DM. Evolutionary deterioration of the vomeronasal pheromone transduction pathway in catarrhine primates. *Proc Natl Acad Sci U S A*. 2003; 100(14):8337–41. <https://doi.org/10.1073/pnas.1331721100> PMID: 12826614
20. Grus WE, Zhang J. Rapid turnover and species-specificity of vomeronasal pheromone receptor genes in mice and rats. *Gene*. 2004; 340(2):303–12. <https://doi.org/10.1016/j.gene.2004.07.037> PMID: 15475172
21. Shi P, Bielawski JP, Yang H, Zhang Y-P. Adaptive diversification of vomeronasal receptor 1 genes in rodents. *J Mol Evol*. 2005; 60(5):566–76.
22. Shi P, Zhang J. Comparative genomic analysis identifies an evolutionary shift of vomeronasal receptor gene repertoires in the vertebrate transition from water to land. *Genome Res*. 2007; 17(2):166–74. <https://doi.org/10.1101/gr.6040007> PMID: 17210926
23. Grus WE, Zhang J. Origin of the genetic components of the vomeronasal system in the common ancestor of all extant vertebrates. *Mol Biol Evol*. 2009; 26(2):407–19. <https://doi.org/10.1093/molbev/msn262> PMID: 19008528
24. Grus WE, Zhang J. Origin and evolution of the vertebrate vomeronasal system viewed through system-specific genes. *Bioessays*. 2006; 28(7):709–18. <https://doi.org/10.1002/bies.20432> PMID: 16850401
25. Grus WE, Shi P, Zhang J. Largest vertebrate vomeronasal type 1 receptor gene repertoire in the semi-aquatic platypus. *Mol Biol Evol*. 2007; 24(10):2153–7. <https://doi.org/10.1093/molbev/msm157> PMID: 17666439
26. Young JM, Trask BJ. V2R gene families degenerated in primates, dog and cow, but expanded in opossum. *Trends Genet*. 2007; 23(5):212–5. <https://doi.org/10.1016/j.tig.2007.03.004> PMID: 17382427
27. Young JM, Massa HF, Hsu L, Trask BJ. Extreme variability among mammalian V1R gene families. *Genome Res*. 2010; 20(1):10–8. <https://doi.org/10.1101/gr.098913.109> PMID: 19952141
28. Young JM. Divergent V1R repertoires in five species: Amplification in rodents, decimation in primates, and a surprisingly small repertoire in dogs. *Genome Res* 2005; 15(2):231–40. <https://doi.org/10.1101/gr.3339905> PMID: 15653832
29. Lane RP, Cutforth T, Axel R, Hood L, Trask BJ. Sequence analysis of mouse vomeronasal receptor gene clusters reveals common promoter motifs and a history of recent expansion. *Proc Natl Acad Sci*. 2002; 99(1):291–6. <https://doi.org/10.1073/pnas.012608399> PMID: 11752409
30. Lane RP, Young J, Newman T, Trask BJ. Species specificity in rodent pheromone receptor repertoires. *Genome Res*. 2004; 14(4):603–8. <https://doi.org/10.1101/gr.2117004> PMID: 15060001
31. Yang H, Shi P, Zhang Y-P, Zhang J. Composition and evolution of the V2r vomeronasal receptor gene repertoire in mice and rats. *Genomics*. 2005; 86(3):306–15. <https://doi.org/10.1016/j.ygeno.2005.05.012> PMID: 16024217
32. Couger MB, Arévalo L, Campbell P. A high quality genome for mus spicilegus, a close relative of house mice with unique social and ecological adaptations. *G3*. 2018; 8(7):2145–52. <https://doi.org/10.1534/g3.118.200318> PMID: 29794166
33. Grus WE, Shi P, Zhang YP, Zhang J. Dramatic variation of the vomeronasal pheromone receptor gene repertoire among five orders of placental and marsupial mammals. *Proc Natl Acad Sci*. 2005; 102(16):5767–72. <https://doi.org/10.1073/pnas.0501589102> PMID: 15790682
34. Duyck K, DuTell V, Ma L, Paulson A, Yu CR. Pronounced strain-specific chemosensory receptor gene expression in the mouse vomeronasal organ. *BMC Genomics*. 2017; 18(1):965. <https://doi.org/10.1186/s12864-017-4364-4> PMID: 29233099
35. Meijer JH, Robbers Y. Wheel running in the wild. *Proc Biol Sci*. 2014; 281(1786). <https://doi.org/10.1098/rspb.2014.0210> PMID: 24850923
36. Sherwin CM. Voluntary wheel running: a review and novel interpretation. *Anim Behav*. 1998; 56(1):11–27. <https://doi.org/10.1006/anbe.1998.0836> PMID: 9710457
37. Garland T Jr., Schutz H, Chappell MA, Keeney BK, Meek TH, Copes LE, et al. The biological control of voluntary exercise, spontaneous physical activity and daily energy expenditure in relation to obesity: human and rodent perspectives. *The Journal of experimental biology*. 2011; 214(Pt 2):206–29. <https://doi.org/10.1242/jeb.048397> PMID: 21177942
38. Novak CM, Burghardt PR, Levine JA. The use of a running wheel to measure activity in rodents: relationship to energy balance, general activity, and reward. *Neuroscience and biobehavioral reviews*. 2012; 36(3):1001–14. <https://doi.org/10.1016/j.neubiorev.2011.12.012> PMID: 22230703

39. Lightfoot JT, EJC DEG, Booth FW, Bray MS, DENH M, Kaprio J, et al. Biological/Genetic Regulation of Physical Activity Level: Consensus from GenBioPAC. *Med Sci Sports Exerc.* 2018; 50(4):863–73. <https://doi.org/10.1249/MSS.0000000000001499> PMID: 29166322
40. Rhodes JS, Gammie SC, Garland T Jr. Neurobiology of mice selected for high voluntary wheel-running activity. *Integrative and comparative biology.* 2005; 45(3):438–55. <https://doi.org/10.1093/icb/45.3.438> PMID: 21676789
41. Claghorn GC, Thompson Z, Wi K, Van L, Garland T Jr., Caffeine stimulates voluntary wheel running in mice without increasing aerobic capacity. *Physiol Behav.* 2017; 170:133–40. <https://doi.org/10.1016/j.physbeh.2016.12.031> PMID: 28039074
42. Drickamer LC, Evans TR. Chemosignals and activity of wild stock house mice, with a note on the use of running wheels to assess activity in rodents. *Behav Processes.* 1996; 36(1):51–66. [https://doi.org/10.1016/0376-6357\(95\)00015-1](https://doi.org/10.1016/0376-6357(95)00015-1) PMID: 24896417
43. Swallow JG, Carter PA, Garland T Jr. Artificial selection for increased wheel-running behavior in house mice. *Behav Genet.* 1998; 28(3):227–37. <https://doi.org/10.1023/a:1021479331779> PMID: 9670598
44. Wallace IJ, Garland T Jr. Mobility as an emergent property of biological organization: Insights from experimental evolution. *Evol Anthropol.* 2016; 25(3):98–104. <https://doi.org/10.1002/evan.21481> PMID: 27312181
45. Kolb EM, Kelly SA, Garland T Jr. Mice from lines selectively bred for high voluntary wheel running exhibit lower blood pressure during withdrawal from wheel access. *Physiol Behav.* 2013; 112–113:49–55. <https://doi.org/10.1016/j.physbeh.2013.02.010> PMID: 23458632
46. Careau V, Wolak ME, Carter PA, Garland T. Limits to behavioral evolution: the quantitative genetics of a complex trait under directional selection. *Evolution.* 2013; 67(11):3102–19. <https://doi.org/10.1111/evo.12200> PMID: 24151996
47. Dewan I, Garland T, Hiramatsu L, Careau V. I smell a mouse: indirect genetic effects on voluntary wheel-running distance, duration and speed. *Behavior Genetics.* 2019; 49(1):49–59. <https://doi.org/10.1007/s10519-018-9930-2> PMID: 30324246
48. Kream RM, Margolis FL. Olfactory marker protein: turnover and transport in normal and regenerating neurons. *J Neurosci.* 1984; 4(3):868–79. <https://doi.org/10.1523/JNEUROSCI.04-03-00868.1984> PMID: 6707736
49. Xu S, Garland T. A mixed model approach to genome-wide association studies for selection signatures, with application to mice bred for voluntary exercise behavior. *Genetics.* 2017; 207(2):785–99. <https://doi.org/10.1534/genetics.117.300102> PMID: 28774881
50. Khan M, Vaes E, Mombaerts P. Regulation of the probability of mouse odorant receptor gene choice. *Cell.* 2011; 147(4):907–21. <https://doi.org/10.1016/j.cell.2011.09.049> PMID: 22078886
51. Hillis DA, Yadgary L, Weinstock GM, Pardo-Manuel de Villena F, Pomp D, Fowler AS, et al. Genetic Basis of Aerobically Supported Voluntary Exercise: Results from a Selection Experiment with House Mice. *Genetics.* 2020. <https://doi.org/10.1534/genetics.120.303668> PMID: 32978270
52. Kolb EM, Rezende EL, Holness L, Radtke A, Lee SK, Obenaus A, et al. Mice selectively bred for high voluntary wheel running have larger midbrains: support for the mosaic model of brain evolution. *The Journal of experimental biology.* 2013; 216(3):515–23. <https://doi.org/10.1242/jeb.076000> PMID: 23325861
53. Swallow JG, Rhodes JS, Garland T Jr. Phenotypic and evolutionary plasticity of organ masses in response to voluntary exercise in house mice. *Integr Comp Biol.* 2005; 45(3):426–37. <https://doi.org/10.1093/icb/45.3.426> PMID: 21676788
54. Kelly SA, Gomes FR, Kolb EM, Malisch JL, Garland T Jr. Effects of activity, genetic selection and their interaction on muscle metabolic capacities and organ masses in mice. *The Journal of experimental biology.* 2017; 220(Pt 6):1038–47. <https://doi.org/10.1242/jeb.148759> PMID: 28096432
55. Kolb EM, Kelly SA, Middleton KM, Sermsakdi LS, Chappell MA, Garland T. Erythropoietin elevates but not voluntary wheel running in mice. 2010; 213(3):510–9. <https://doi.org/10.1242/jeb.029074> PMID: 20086137
56. Kay JC, Claghorn GC, Thompson Z, Hampton TG, Garland T Jr. Electrocardiograms of mice selectively bred for high levels of voluntary exercise: Effects of short-term exercise training and the mini-muscle phenotype. *Physiol Behav.* 2019; 199:322–32. <https://doi.org/10.1016/j.physbeh.2018.11.041> PMID: 30508549
57. Rezende EL, Gomes FR, Malisch JL, Chappell MA, Garland T Jr. Maximal oxygen consumption in relation to subordinate traits in lines of house mice selectively bred for high voluntary wheel running. *J Appl Physiol.* 2006; 101(2):477–85. <https://doi.org/10.1152/jappphysiol.00042.2006> PMID: 16601309
58. Haga S, Hattori T, Sato T, Sato K, Matsuda S, Kobayakawa R, et al. The male mouse pheromone ESP1 enhances female sexual receptive behaviour through a specific vomeronasal receptor. *Nature.* 2010; 466(7302):118–22. <https://doi.org/10.1038/nature09142> PMID: 20596023

59. Ferrero DM, Moeller LM, Osakada T, Horio N, Li Q, Roy DS, et al. A juvenile mouse pheromone inhibits sexual behaviour through the vomeronasal system. *Nature*. 2013; 502(7471):368–71. <https://doi.org/10.1038/nature12579> PMID: 24089208
60. Cheetham SA, Smith AL, Armstrong SD, Beynon RJ, Hurst JL. Limited variation in the major urinary proteins of laboratory mice. *Physiol Behav*. 2009; 96(2):253–61. <https://doi.org/10.1016/j.physbeh.2008.10.005> PMID: 18973768
61. Rhodes JS, Garland T Jr., Gammie SC. Patterns of brain activity associated with variation in voluntary wheel-running behavior. *Behav Neurosci*. 2003; 117(6):1243–56. <https://doi.org/10.1037/0735-7044.117.6.1243> PMID: 14674844
62. King JM. Effects of lesions of the amygdala, preoptic area, and hypothalamus on estradiol-induced activity in the female rat. *Journal of comparative and physiological psychology*. 1979; 93(2):360–7. <https://doi.org/10.1037/h0077559> PMID: 457955
63. Fahrbach S, Meisel R, Pfaff D. Preoptic implants of estradiol increase wheel running but not the open field activity of female rats. 1985; 35(6):985–92. [https://doi.org/10.1016/0031-9384\(85\)90270-7](https://doi.org/10.1016/0031-9384(85)90270-7) PMID: 4095192
64. Ogawa S, Chan J, Gustafsson J-Å, Korach KS, Pfaff DW. Estrogen Increases Locomotor Activity in Mice through Estrogen Receptor  $\alpha$ : Specificity for the Type of Activity. *Endocrinology*. 2003; 144(1):230–9. <https://doi.org/10.1210/en.2002-220519> PMID: 12488349
65. Spiteri T, Ogawa S, Musatov S, Pfaff DW, Ågmo A. The role of the estrogen receptor  $\alpha$  in the medial preoptic area in sexual incentive motivation, proceptivity and receptivity, anxiety, and wheel running in female rats. 2012; 230(1):11–20.
66. Dobin A, Davis CA, Schlesinger F, Drenkow J, Zaleski C, Jha S, et al. STAR: ultrafast universal RNA-seq aligner. *Bioinformatics*. 2013; 29(1):15–21. <https://doi.org/10.1093/bioinformatics/bts635> PMID: 23104886
67. Trapnell C, Hendrickson DG, Sauvageau M, Goff L, Rinn JL, Pachter L. Differential analysis of gene regulation at transcript resolution with RNA-seq. *Nat Biotechnol*. 2013; 31(1):46–53. <https://doi.org/10.1038/nbt.2450> PMID: 23222703
68. Bankhead P, Loughrey MB, Fernandez JA, Dombrowski Y, McArt DG, Dunne PD, et al. QuPath: Open source software for digital pathology image analysis. *Sci Rep*. 2017; 7(1):16878. <https://doi.org/10.1038/s41598-017-17204-5> PMID: 29203879